Soc. Extended Abst. 1984, 2, 897.
(14) Elsenbaumer, R. L.; Miller, G. G.; Khanna, Y. P.; McCarthy, E.; Baughman, R. H. Electrochem. Soc. Extended Abst. 1985, 1, 118.
(15) Diaz, A. F.; Hall, B. IBM J. Res. Dev. 1983 27, 342.
(16) Druy, M. A. J. Electrochem. Soc., in press.
(17) Druy, M. A.; Seymour, R. J.; Tripathy, S. K. ACS Symp. Ser. 1984, No. 242, 473.
(18) Salmon, M.; Diaz, A. F.; Logan, A. J.; Krounbi, M.; Bargon, J. Mol. Cryst. Liq. Cryst. 1982, 83, 265.

Experimental Study of the Density Recovery of Pressure-Densified Polystyrene Glasses

Gary J. Kogowski† and F. E. Filisko*

Department of Materials and Metallurgical Engineering and Macromolecular Research Center, The University of Michigan, Ann Arbor, Michigan 48109. *Received July 23, 1985*

ABSTRACT: Densities were measured vs. time at various annealing temperatures (65, 80, and 95 °C) for polystyrene glasses vitrified at various pressures and cooling rates. Results show that the rate of density change at early times is much more rapid for samples formed at high pressures and cooling rates. A minimum density or "undershoot" was observed, the magnitude of which increased with vitrification pressure and cooling rate. For each annealing temperature, all samples attained the same constant density at long times, independent of vitrification conditions. Samples vitrified at atmospheric pressure, despite the initially greater free volume and smallest displacement from equilibrium, recovered slowest and took longer to reach these constant densities. Densities were measured by density gradient columns at 23 °C.

Introduction

Measurements of density or specific volume with time are a common means to characterize physical aging or recovery of polymeric glasses below T_g.[1-5] In most experiments, the material is subjected to various thermal histories or annealing treatments prior to measurements. Indeed, the temperature-jump experiments of Kovacs[3] and subsequent theories to describe volume changes with time provide valuable insight into the volume-recovery mechanism.[6-13] Density, however, is affected not only by thermal history but to a greater extent by solidification pressure.[14-20] The effect of pressure on recovery rate is important from a theoretical viewpoint by presenting data that will allow a greater refinement of current theories and from a practical viewpoint because processing methods like injection molding involve materials solidifying under elevated pressure. It is well established that applied pressure changes the glass transition temperature, and subsequent cooling of the materials through T_g while under applied pressure significantly affects volume recovery. In this report we investigate the effects of solidification pressure and cooling rate on the aging of glassy polystyrene at atmospheric pressure.

In the pressure-step experiment the glass is cooled from the liquid state through the glass transition temperature under hydrostatic pressure. When the glass attains ambient temperature, the pressure is suddenly released. Following the depressurization step, the glasses are annealed at temperatures near the glass transition temperature. The changes in density occurring during the annealing process are measured by density gradient column at 23 °C.

Density gradient columns were used because they allowed us to use very small samples, thus minimizing density inhomogeneities within the samples and time to reach thermal equilibrium before meaningful measurements could be made. This is particularly important because recovery can occur rapidly within the first few minutes for some sample preparations.

†Present address: Allied Corporation, Automotive Division, Troy, Michigan.

Experimental Section

Materials. The polystyrene used was a Dow special additive-free grade in the form of transparent pellets. The pellets measured about 3 mm in length and 1.5 mm in diameter. Each pellet weighed about 30 mg with MW = 3.1×10^5 and M_w/M_n = 2.78 as determined by GPC analysis.

Equipment. Pressure-densified glasses were prepared with the apparatus diagrammatically illustrated in Figure 1. The pressure source was a Teledyne-Sprague Engineering high-pressure, air-driven hydraulic pump (No. s-216-cs-700-ss), which was capable of 500 MPa from a 0.7-MPa air line. Samples in pellet form were individually wrapped in Teflon tape, stacked into the high-pressure cylinder, and covered with purified mercury. A resistance heating jacket was placed around the cylinder and connected to a controller–power supply. A thermocouple used for temperature control was placed into a small hole drilled directly into the pressure vessel. Temperature control and cooling rate programming were accomplished by an Omega Engineering Model 49 proportioning control unit that was connected to an R.I. Controls Model FGE 5110 Data-Trak cooling rate controller.

Three annealing ovens were set up for long-term annealing (24 h to 1 year) at the following temperatures, 95 °C (±0.14 °C) (Ransco Industry temperature test chamber no. SD 30-1), 80 °C (±0.5 °C) (Central Stabil-Therm constant-temperature cabinet), and 65 °C (±0.5 °C) (Central Scientific Co. constant-temperature appliance, no. 98308).

A specially modified oven (Delta Design Inc. temperature test chamber Model No. 6545-S) was used for short-term annealing (70 s to 24 h). This oven allowed quick removal of the samples required for short annealing time. Samples were annealed at the same temperatures stated above, i.e., 95, 80, and 65 °C.

Approximately 30 pellets were compressed per pressurization experiment. These samples were compressed at ambient temperature and heated 10–20 °C above the glass transition temperature calculated for each pressure. The sample remained compressed at least 45 min to allow it to equilibrate. The applied pressures used were atmospheric, 69 MPa (10 000 psi), 138 MPA (20 000psi), 207 MPA (30 000psi), and 276 MPa (40 000 psi). The two cooling rates used were 3.3×10^{-3} °C/s (slow-cooled) and 5 °C/s, obtained by fast-cooling into ice water. In either case the samples were cooled to about 23 °C, and the pressure was released. The densified glasses were unwrapped, placed into a Buchner funnel, and washed with cold distilled water. After the samples were cleaned, they were placed into a Sorvall superspeed angled centrifuge (Type SS-1-A) and spun in a low-density cold sodium bromide solution. This procedure helped eliminate air from any microcracks in the surface of the samples and resulted in precise

0024-9297/86/2219-0828$01.50/0

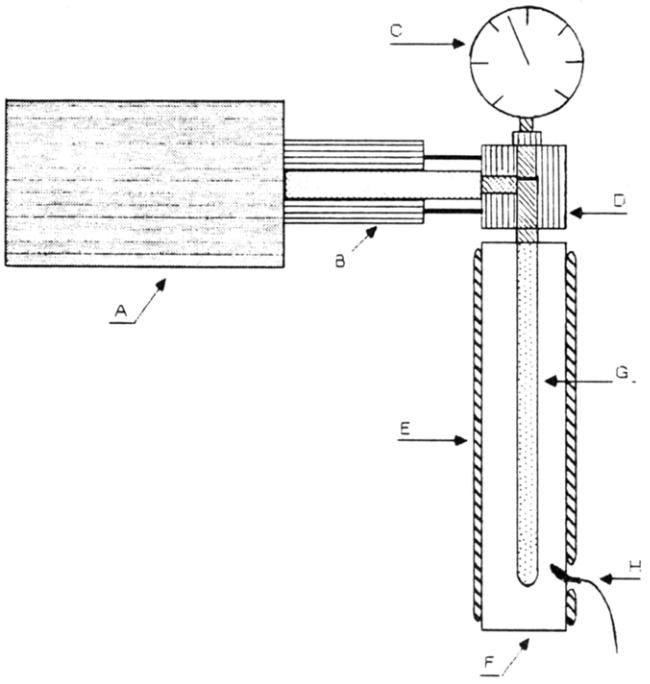

Figure 1. Schematic of high-pressure pump and pressure vessel: (A) high-pressure pump; (B) piston and housing assembly; (C) pressure gauge; (D) fluid line and connector; (E) heating jacket; (F) high-pressure cell; (G) pressure chamber with sample; (H) thermocouple.

density measurements. To ensure that negligible changes occurred at room temperature with the samples following both the pressurization and annealing sequences, measurements were made as rapidly as possible (about 2 h) after removal of the samples from the pressure vessels or ice water quenching from the annealing temperatures. This was further determined by observing samples in the column (at 23 °C) for a 2-week period, over which time no significant density changes occurred.

Density Column Preparation. Densities of the samples were measured in density gradient columns prepared according to ASTM Standard D 1505-68, method C. The columns were made with deaerated distilled water–sodium bromide solutions. Each column was calibrated with 5 calibrated glass density beads (purchased from Techne Inc., Princeton, NJ) ranging in density from 1.0300 to 1.0805 g/cm^3. All densities were measured at 23.0 °C (±0.05 °C).

Three columns were prepared, one for each annealing temperature, and calibrations were checked during each day of operation. Resulting column calibrations were linear and had a correlation coefficient of at least −0.99998 based on linear regression analysis (HP 15C calculator) of the reference standard density beads vs. bead height (mm). Columns retained good correlation for 6–8 weeks. After this time or when the correlation coefficient decayed to −0.998, the columns were discarded.

Measurements of Pressure-Densified Glasses. For each pressure and cooling rate at least 125 pellet-size pressure-densified samples were dropped into the columns. After the densities of these samples were recorded, they were removed from the columns, rinsed with cold distilled water, air-dried, and placed into annealing ovens.

To determine the minimum time required for a pellet to attain uniform temperature for annealing, a thermojunction was embedded into a liquid pellet and allowed to vitrify. The reference junction was placed into a 0 °C ice bath. The pellet was raised to 140 °C until thermal equilibrium was attained, as indicated by a level base line on a strip-chart recorder. The pellet was fast-cooled to sub-T_g temperatures, and the time required for a stable base line to be attained was calculated. Results indicate that 45–60 s was required for the pellet to become uniformly heated.

Pressure-Densified Annealed Samples. Long-term annealed samples were wrapped with aluminum foil, placed in petri dishes, covered with Dryrite, and placed into annealing ovens. Short-term annealed samples were held by alligator clips that were soldered to the end of a long wire and inserted into the short-term oven heating chamber through tubes made of copper.

At the end of a specified annealing time the samples were removed from the ovens and fast-cooled into cold distilled water. The samples were centrifuged and placed in the gradient column. In the column, densities were measured at times ranging from 20 min to 24 h. In all cases no change occurred in density after 2 h. Recovery data were reproduced with at least four annealed sample measurements per point.

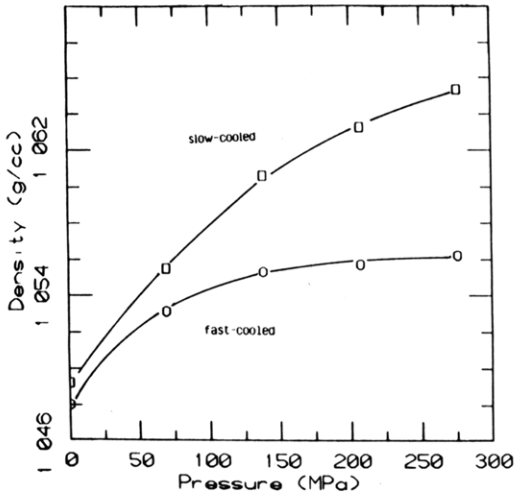

Figure 2. Density behavior as a function of pressure for the two cooling rates used in these experiments. The glass fast-cooled through the glass transition temperature levels off at an earlier time.

Table I

	density, g/cm^3	
pressure, MPa	fast-cool, 5 °C/s	slow-cool, 3.3 × 10^{-3} °C/s
atmospheric[a]	1.0479 (±0.0001)	1.0492 (±0.0001)
69	1.0531 (±0.0003)	1.0555 (±0.0004)
138	1.0553 (±0.0002)	1.0606 (±0.0004)
207	1.0557 (±0.0003)	1.0633 (±0.0004)
276	1.0562 (±0.0003)	1.0654 (±0.0004)

[a] Density when medium-cooled (3.3 × 10^{-2} °C/s) at atmospheric pressure is 1.0488 (±0.0005) g/cm^3.

Results

Formation Densities. The densities of polystyrene at 23 °C and atmospheric pressure after cooling through the glass transition temperature at different elevated pressures and cooling rates are shown in Figure 2. The data are shown in Table I.

The density of slow-cooled pressure-densified glasses increases rapidly with pressure at low pressures and shows a tendency toward leveling off at high pressures. The density of the fast-cooled pressure-densified glasses shows a slight increase above 138 MPa and should become constant in the range 275–350 MPa, some 200 MPa less than for slow-cooled glasses. (It should be mentioned that the formation of glasses under vacuum (33 Pa) was attempted. The intitial densities were the same as those for the atmospheric-pressure-densified glasses.)

Density changes of the pressure-densified glasses annealed at 65 °C and slow-cooled through the glass transition temperature are shown in Figure 3. At this annealing temperature and cooling rate the density of the glass vitrified at 276 MPa approaches equilibrium fastest even though it is farthest removed from equilibrium. The glasses densified at 207 and 138 MPa exhibit slower density changes, but these changes are parallel to those exhibited

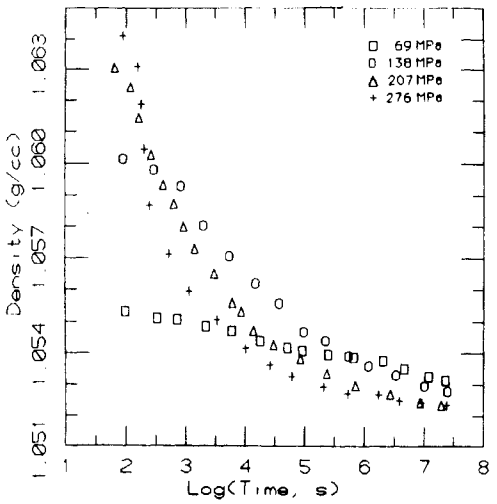

Figure 3. Changes in density of pressure-densified glasses annealed at 65 °C and slow-cooled through the glass transition temperature. Density is approaching a constant value at long time periods.

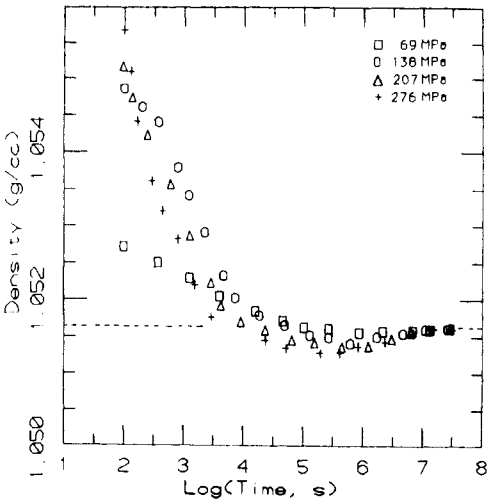

Figure 4. Changes in density of pressure-densified glasses annealed at 65 °C and fast-cooled through the glass transition temperature. Constant density is attained at about 1 year at this annealing temperature and cooling rate. The dashed line indicates the extrapolation of constant density.

by the glass vitrified at 276 MPa. Although the densities of these three pressure-densified glasses decrease at varying rates at early annealing time, they cross at approximately the same density (1.060 g/cm^3). The changes in density appear to be approaching a constant density at longer annealing time. The glass densified at 69 MPa recovers slowest. The density of this glass crosses the other pressure-densified glasses at about 1 h and becomes coincident with them after about 500 h.

Figure 4 shows the density changes of glasses densified at 276, 207, 138, and 69 MPa that were fast-cooled through T_g and annealed at 65 °C. Density changes are similar to but much faster than those of the slow-cooled pressure-densified glasses annealed at the same temperature (65 °C). The 276-MPa-densified glass recovers fastest followed by the 207- and 138-MPa-densified glasses. The crossover point occurs at the same time as for the slow-cooled glasses (3 min), but the density is lower (1.0545 g/cm^3), reflecting a faster kinetic process. The density of the 69-MPa-densified glass again crosses those of others but becomes coincident with them after about 10 h of annealing time, 490 h sooner than those of the slow-cooled densified glasses annealed at the same temperature. These glasses also

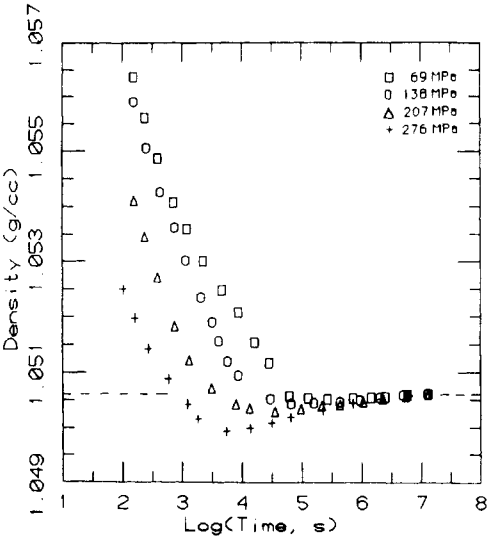

Figure 5. Changes in density of pressure-densified glasses annealed at 80 °C and slow-cooled through the glass transition temperature. Density recovery is nearly parallel at early time. Constant density is attained at about 100 h. The dashed line indicates the extrapolation of constant density.

attain a constant density in about 8800 h (1 year).

The density changes of the pressure-densified glasses slow-cooled through T_g and annealed at 80 °C are shown in Figure 5. Clearly the initial densities of the samples at zero time should be highest at high pressure and lowest for samples vitrified at 69 MPa. The reverse order is indicated here. This simply means that the high-pressure-densified samples annealed most rapidly and the low-pressure-densified samples annealed most slowly in the initial 100 s of annealing for which the densities were not obtained. A density minimum is observed at this annealing temperature and cooling rate that is similar to that of the pressure-densified glasses annealed at 65 °C and fast-cooled through the glass transition temperature. The undershoot ranges from 0.1 to 100 h, which is a much shorter time span than the undershoot observed for the 65 °C annealed fast-cooled glasses (1–500 h). A constant density is attained after about 1000 h, some 7800 h before that of the glasses annealed at 65 °C and fast-cooled through T_g.

The samples vitrified at 69 and 138 MPa show unusual recovery in that they do not appear to exhibit exponential behavior. Around 10^5 s, an inflection point exists followed by immediate attainment of equilibrium. This behavior should not occur unless the density undershoot is shifted to earlier times. This seems to be the case. At lower pressures the recovery rate is slower than for the higher-pressure-densified samples and a slight bulge is observed around 10^4 s. This bulge is the density overshoot exhibited by the higher-pressure-densified glasses. The overshoot is simply shifted to shorter times and has a much smaller magnitude than the corresponding higher-pressure-densified glasses.

Figure 6 shows the density change of the glasses that were annealed at 80 °C but fast-cooled through the glass transition temperature. Density recovery is consistent with the 80 °C annealed slow-cooled glasses; i.e., the 276-MPa-densified glass decreases in density the fastest, followed by the 207-, 138-, and 69-MPa-densified glasses. The undershoot again appears at this cooling rate but has more depth and a slightly smaller time range than the glasses slow-cooled through T_g and annealed at the same temperature (80 °C). Constant density is attained at the same time as for the slow-cooled glasses, about 1000 h, and the

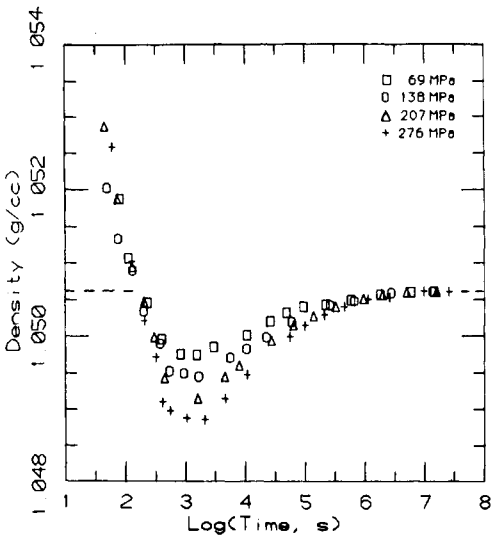

Figure 6. Changes in density of pressure-densified glasses annealed at 80 °C and fast-cooled through the glass transition temperature. The density undershoot has more depth at this cooling rate and temperature. The dashed line indicates the extrapolation of constant density.

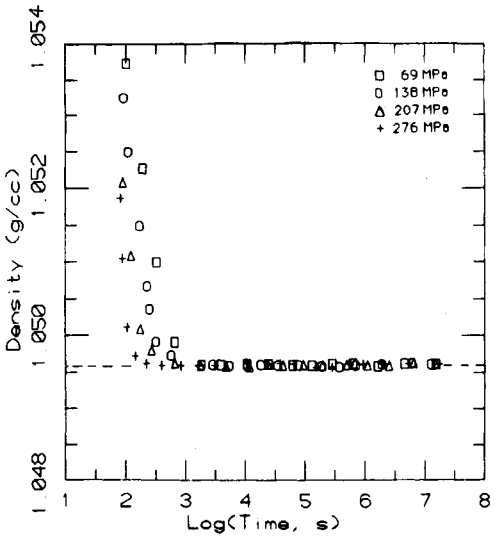

Figure 7. Changes in density of pressure-densified glasses annealed at 95 °C and slow-cooled through the glass transition temperature. Constant density is attained in less than 1 h.

same density is attained as that of the corresponding slow-cooled glasses at the same annealing temperature.

Figures 7 and 8 show the density-recovery behavior of both the slow-cooled and fast-cooled glasses annealed at 95 °C. The density decreases at a rate much faster than either 65 or 80 °C annealed glasses. The undershoot is also observed at this annealing temperature but at an earlier annealing time (<1 h). The undershoot is shallow and appears to range only a few minutes. The same constant density is attained for both cooling rates and occurs at about 0.9 h, some 1100 times faster than for the glasses annealed at 80 °C. Consistent with previous data, the density of the 276-MPa-formed glass decreases fastest even though it is farthest removed from equilibrium, while the density of the 69-MPa-formed glass decreases slowest.

The increase in density of the glasses densified at atmospheric pressure, slow-cooled or fast-cooled through the glass transition temperature, and annealed at 95 °C is shown in Figure 9. In this figure the pressure-densified curves for the slow-cooled samples are shown for comparison. The atmospheric-pressure-densified glasses show

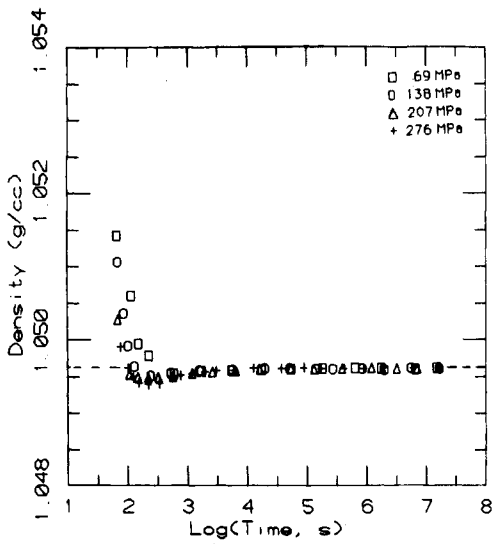

Figure 8. Changes in density of pressure-densified glasses annealed at 95 °C and fast-cooled through the glass transition temperature. The dashed line indicates the extrapolation of constant density.

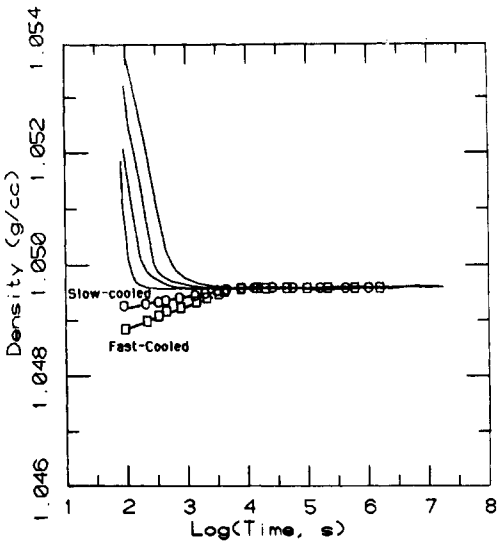

Figure 9. Changes in density of atmospheric pressure densified glasses annealed at 95 °C. Both fast- and slow-cooling rates through the glass transition temperature are shown. Pressure-densified glasses annealed at the same temperature and slow-cooled through T_g are shown for comparison.

Table II

constant density,[a] cm^2	annealing temp, °C
1.0517	65.0
1.0506	80.0
1.0496	95.0

[a] Measured at 23 °C.

significantly slower density changes than the corresponding pressure-densified glasses at the same annealing temperature and cooling rate. Equilibrium is attained at about 900 h. Atmospheric-pressure-densified glasses annealed at 80 and 65 °C (not shown here) follow the same general recovery kinetics as the glasses annealed at 95 °C, but recovery is much slower. Equilibrium was attained for the glasses annealed at 80 °C at about 1 year. The glasses annealed at 65 °C did not attain equilibrium after 1 year of annealing.

The constant density attained at each annealing temperature (measured at 23 °C) is shown in Figure 10, and experimental data are given in Table II. Densities of the

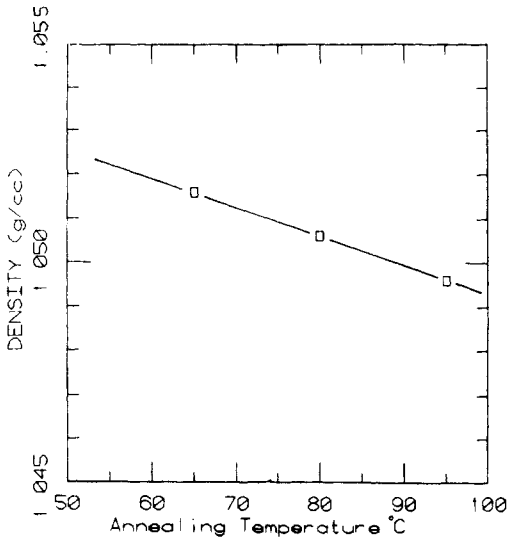

Figure 10. Constant density as a function of annealing temperature. A linear relationship is observed irrespective of cooling rate through the glass transition temperature and vitrification pressure.

65 °C annealed glasses that were slow-cooled through the glass transition temperature are not included because they did not attain equilibrium.

Method. Density column calibration was analyzed by least-squares analysis, and the results were used directly to calculate the sample's gradient of 8×10^{-4} g/cm^3 per centimeter of length of column. Column position could be measured precisely to a resolution of 0.01 cm. Therefore density differences of 8×10^{-6} g/cm^3 should be measureable. Problems in visually determining the center of mass of the specimen reduced the resolution to approximately 3×10^{-4} g/cm^3. Deviations greater than this value for a particular glass may not be due to procedural error but might result from inhomogeneities in the samples. The significance of these deviations are best judged when the total range of observable densities and the precision required of the analysis to be performed are known. Previously described errors such as selective absorption of one liquid component and incomplete wetting have been virtually eliminated by the centrifugation process.[19] Among the advantages of the gradient method are easy calibration, small samples, and long life span. The small sample size was an essential part of this study, which was to acquire significant recovery data at times as low as possible.

Comparisons with Previous Data. The kinetics of density recovery for these pressure-densified glasses are unique and cannot directly be compared to other reported data. However, we can compare the times that constant density (equilibrium) is attained for each annealing temperature. Kovacs reported volume-recovery data for polystyrene glasses that were cooled from the liquid state (at atmospheric pressure) and then annealed at different temperatures below T_g (single temperature step).[2] For glasses annealed at 90 °C, Kovacs reported equilibrium was attained in about 1 h (these data, of course, do not show maxima). The pressure-densified glasses reported here attain equilibrium at slightly less than 1 h. At a lower annealing temperature, 80 °C, Kovacs reported equilibrium was not attained before 100 h, and extrapolation shows that equilibrium is attained at about 1000 h. Our data show that glasses annealed at 80 °C attain equilibrium between 850 and 1000 h, which is on the similar time scale for atmospheric samples previously reported by Kovacs. Kovacs reported that polystyrenes annealed at 60 and 70 °C are not near equilibrium after 100 h. Extrapolation of his data indicates that at least 2 more decades of time are required for samples to attain equilibrium. Our results show that the slow-cooled pressure-densified glasses annealed at 65 °C do not attain equilibrium within 1 year (8700 h). The pressure-densified glasses fast-cooled through T_g and annealed at 65 °C likely attain equilibrium after 1 year.

Density-Recovery Data. Density recovery of the pressure-densified glasses studied in these experiments exhibits the following features: (1) the density decreases to a minimum at early annealing times and then slowly increases, approaching a constant value; (2) as the annealing temperature increases, density minima become more pronounced and occur at shorter times; (3) as the rate of cooling through the glass transition temperature increases, the breadth of the density minima narrows; (4) as the vitrification pressure and cooling rate increase, the depth of the density minima increases.

The glasses that were densified at the highest pressure (276 MPa) are farther removed from equilibrium at zero time than the glasses densified at lower pressures. However, these glasses attain density minima fastest and approach equilibrium coincident with the others at longer annealing time. This behavior also occurs for the glasses densified at 207 and 138 MPa, which are farther removed from equilibrium than the glasses densified at 69 MPa. The glasses densified at the lowest pressure (69 MPa) are closest to equilibrium but approach equilibrium at rates comparable with the glasses densified at higher pressures. This behavior accounts for the various crossover points observed in the recovery kinetics. If the same kinetic processes were occurring for the various pressure-densified glasses, then the curves could be shifted along the time axis to form a master curve, which clearly cannot be done. This suggests that pressure-densified glasses recover by different mechanisms dependent on the pressurization cycle, reflecting the complex internal structure of the glass imposed by the application and release of pressure.

The occurrence of density minima clearly shows that the volume changes in pressure-densified glasses are not driven solely by the deviation of the total volume from equilibrium. Rather, it indicates that pressure-densified glasses have a complex internal structure and that different parts of the structure respond differently as the pressure is released. Recently, a theoretical glass that had an equilibrium volume with either a narrower or broader free volume distribution was shown to yield maxima or minima in volume during the time development of the glass following its depressurization.[23] The free volume distribution refers to the free volume at different sites scattered throughout the polymer. The maxima and minima exist because regions of higher free volume are first to respond. If the distribution is narrower than the equilibrium distribution, the sites with higher free volume tend (on average) to become sites of even more free volume. Because this occurs before the sites with lower free volume become on average sites with even less free volume, a maximum in volume and a minimum in volume presumably occur as well. This analysis has been applied to the present data, and the detailed results are described in another paper.[24] An alternate explanation is that conformational energies of the macromolecules are of prime importance in the relaxational kinetics. This aspect will be presented also in a subsequent paper.

Acknowledgment. This research was carried out with support from The University of Michigan and from industrial sponsors of the Macromolecular Research Center at The University of Michigan.

Registry No. Polystyrene (homopolymer), 9003-53-6.

References and Notes

(1) Tool, A. Q. *J. Res. Natl. Bur. Stand.* **1946**, *37*, 73.
(2) Kovacs, A. J. *J. Polym. Sci.* **1958**, 131.
(3) Kovacs, A. J. *Adv. Polym. Sci.* **1963**, *3*, 394.
(4) Hozumi, S.; Wakabayashi, T.; Sugihara, K. *Polym. J. (Tokyo)* **1970**, *1*, 632.
(5) Adachi, K.; Kotaka, T. *Polym. J. (Tokyo)* **1982**, *14*, 959.
(6) Kovacs, A. J.; Aklonis, J. J.; Hutchinson, J. M.; Ramon, A. R. *J. Polym. Sci., Polym. Phys. Ed.* **1979**, *17*, 1119.
(7) Kovacs, A. J.; Hutchinson, J. M.; Aklonis, J. J. In "Structure of Non-Crystalline Materials"; Gaskell, P. H., Ed.; Taylor and Francis: London (1977; 153.
(8) Kovacs, A. J. *Ann. N.Y. Acad. Sci.* **1981**, *371*, 38.
(9) Somcynsky, T.; Simha, R. *J. Appl. Phys.* **1971**, *42*, 4545.
(10) Robertson, R. E. *J. Polym. Sci., Polym. Symp.* **1978**, *No. 63*, 173.
(11) Robertson, R. E. *J. Polym. Sci., Polym. Phys. Ed.* **1979**, *17*, 579.
(12) Robertson, R. E. *Ann. N.Y. Acad. Sci.* **1981**, *371*, 21.
(13) Robertson, R. E.; Simha, R.; Curro, J. G. *Macromolecules* **1984**, *17*, 911.
(14) Gee, G. *Polymer* **1966**, *7*, 177.
(15) Goldbach, G.; Rehage, G. *J. Polym. Sci., Part C* **1967**, *16*, 2289.
(16) Quach, A.; Simha, R. *J. Appl. Phys.* **1971**, *42*, 4592.
(17) Price, C.; Williams, R. C.; Ayerst, R. C. In "Amorphous Materials"; Douglas, R. W., Ellis, B., Eds.; Wiley-Interscience: London, 1971; Chapter 12.
(18) Weitz, A.; Wunderlich, B. *J. Polym. Sci., Polym. Phys. Ed.* **1974**, *12*, 2473.
(19) Oels, H.-J.; Rehage, G. *Macromolecules* **1977**, *10*, 1036.
(20) Zehavi, A.; Filisko, F. E. *J. Macromol. Sci., Phys.* **1982**, *B21* (3), 417.
(21) Golba, J., Thesis, The University of Michigan, Ann Arbor, MI, 1979.
(22) Blackadder, D. A.; Henry, J. S. *Makromol. Chem.* **1971**, *141*, 211.
(23) Robertson, R. E.; Simha, R.; Curro, J. G. to be published.
(24) Kogowski, G. J.; Robertson, R. E.; Filisko, F. E. to be published.

Relationship of the Unweighted Rosenbluth and Rosenbluth Walk to a Polymer Chain at the Θ Point

Charles M. Guttman

Polymers Division, National Bureau of Standards, Gaithersburg, Maryland 20899.

Received June 25, 1985

ABSTRACT: It is shown that the unweighted Rosenbluth and Rosenbluth (R–R) chains (sometimes called the "true" self-avoiding walk) can be viewed as polymer chains at the Θ point where only second-order cluster-like terms have been included in the partition function. A modified weighting function for the R–R model is proposed that includes only such second-order cluster terms. Such a polymer chain is shown to show normal polymer chain behavior, i.e., chain expansion, a Θ point, and chain collapse. It is suggested that by comparing the results of studies on these chains with those obtained by a normal R–R weighting procedure one should be able to accurately assess the contributions of third-order and higher order cluster terms to polymer chain properties.

I. Introduction

The self-repelling chain or the "self-avoiding" walk (SAW) has been used to model the equilibrium statistics of linear polymers in dilute solutions of good solvents.[1,2] In such a model one enumerates all configurations of an N-step walk where the walks are not allowed to intersect themselves. For the SAW one obtains measures of the size of the chain that differ from those obtained for a random walk model of the chain. For example, the mean squared radius of gyration, $\langle R_g^2 \rangle$, of a SAW is found to be

$$\langle R_g^2 \rangle = N^{\gamma} \tag{1.1}$$

where γ is about 1.2.

Recently Amit et al.[3] suggested that a random walk in which the traveler steps randomly but tries to avoid places he has already visited be called the "true" self-avoiding random walk (TSAW). They point out that this "true" self-avoiding random walker is very different from the normal self-avoiding random walk used in polymer physics to describe a chain in a good solvent, the SAW. Using renormalization group theory they find that the mean squared end-to-end distance, $\langle R^2 \rangle$, obeys an equation of the form

$$\langle R^2 \rangle \sim N \tag{1.2}$$

They also present Monte Carlo data confirming eq 1.2.

Following the work of Amit et al., a number of similar models have appeared in the literature. Some of them have been related to kinetics of chain growth; others have been related to the growth of polymer gels.[4–6] One such model, the kinetic growth walk (KGW) proposed by Majid et al.,[5] is similar to that of Amit et al. in that it includes self-avoidance in the sense of Amit et al. as well as trapping. For this model Majid et al. do not find that eq 1.2 is exact; rather, they find that the mean squared radius of gyration $\langle R_g^2 \rangle$ of the chain obeys the equation

$$\langle R_g^2 \rangle \sim N(\ln N)^{0.2} \tag{1.3}$$

Here we point out the difference in these walks. In the SAW a walker randomly chooses his next step from among all the nearest-neighbor sites whether they have been visited previously or not; if the walker chooses a visited site, the walk stops. In a TSAW the walker visits all nearest-neighbor sites but chooses among those sites with different probability such that the walk favors unvisited sites; in the TSAW the walker is thus never stopped. In the KGW the walker chooses among only unvisited nearest-neighbor sites with equal probability; the walker is only stopped if all nearest-neighbor sites have been previously visited (called "trapping").

Amit et al. suggested (see their note added in proof) that their "true" self-avoiding random walks are identical with the unweighted form of the chains suggested by Rosenbluth and Rosenbluth[7] (R–R) for use in Monte Carlo simulations of polymer chains.[8] In fact, as a result of trapping, the R–R model is more closely akin to the KGW chain.

Many authors have studied the R–R chains in their context as a generator of the normal excluded volume self-avoiding polymer chains.[7–10] In addition, nearest-